Acta Geochim (2017) 36(4):645–657
DOI 10.1007/s11631-017-0154-6

ORIGINAL ARTICLE

Carbon dioxide emissions from the Three Gorges Reservoir, China

Shuang Li[1] · Fushun Wang[1] · Wenyun Luo[1] · Yuchun Wang[2] · Bing Deng[3]

Received: 10 January 2017 / Revised: 1 March 2017 / Accepted: 27 March 2017 / Published online: 31 March 2017

Abstract Carbon dioxide (CO_2) emission from the river-type reservoir is an hotspot of carbon cycle within inland waters. However, related studies on the different types of reservoirs are still inadequate. Therefore, we sampled the Three Gorges Reservoir (TGR), a typical river-type reservoir having both river and lake characteristics, using an online system (HydroCTM/CO_2) and YSI-6600v2 meter to determine the partial pressure of carbon dioxide (pCO_2) and physical chemical parameters in 2013. The results showed that the CO_2 flux from the mainstream ranged from 26.1 to 92.2 mg CO_2/m^2 h with average CO_2 fluxes of 50.0 mg/m^2 h. The CO_2 fluxes from the tributary ranged from -10.91 to 53.95 mg CO_2/m^2 h with area-weighted average CO_2 fluxes of 11.4 mg/m^2 h. The main stream emits CO_2 to the atmosphere the whole year; however, the surface water of the tributary can sometimes act as a sink of CO_2 for the atmosphere. As the operation of the TGR, the tributary became more favorable to photosynthetic uptake of CO_2 especially in summer. The total CO_2 flux was estimated to be 0.34 and 0.03 Tg CO_2/year from the mainstream and the tributaries, respectively. Our emission rates are lower than previous estimates, but they are in agreement with the average CO_2 flux from temperate reservoirs estimated by Barros et al. (Nat Geosci 4(9):593–596, 2011).

Keywords CO_2 emissions · Three Gorges Reservoir · River-type reservoir

1 Introduction

The river systems have a major biogeochemical role in the global carbon cycle because they export the total organic and inorganic carbon from the terrestrial environment to the ocean (Zhao et al. 2012). Actually, river systems can also exchange CO_2 with the atmosphere at the water–air interface. Early estimates suggested that the outgassing amount is 1.2 $\pm$ 0.3 MgC/ha yr as CO_2 from rivers and wetlands of the central Amazon Basin (Richey et al. 2002). According to conservative estimates, the terrestrial landscape input 1.9 Pg C/y to inland waters, of which about 0.2 Pg C/y is buried in aquatic sediments, 0.9 Pg C/y is delivered to the oceans, while at least 0.8 Pg C/y is returned to the atmosphere via gas exchange (Cole et al. 2007). According to recent estimates by Raymond, 1.8 Pg C/year from streams and rivers was released into the atmosphere (Raymond et al. 2013). The carbon emission estimates from river systems has counter-balanced the terrestrial carbon sink and thus deserve attention. However, these global estimates still have a lot of uncertainty due to limited data, bias in data distribution, and difficulties in assigning specific areas for upscaling to specific types of inland waters. More importantly, a comprehensive body of published data reveals that human activities have greatly changed the carbon exchange between land, freshwater bodies, the atmosphere and the ocean (Regnier et al. 2013). For example, terrestrial land can convert to an aquatic area

✉ Fushun Wang
lishuang710@qq.com; fswang@shu.edu.cn

[1] School of Environmental and Chemical Engineering, Shanghai University, Shanghai 200444, China

[2] Department of Water Environment, China Institute of Water Resources and Hydroelectric Power Research, Beijing 100038, China

[3] State Key Laboratory of Estuarine and Coastal Research, East China Normal University, Shanghai 200633, China

after a reservoir impoundment, bringing with this conversion the related issues of greenhouse gas (GHG) emission and carbon cycle change (St. Louis et al. 2000). The research results have shown that CO_2 emissions from reservoir surfaces account for approximately 4% of all anthropogenic sources (Barros et al. 2011; Kemenes et al. 2011). Thus, the human-induced carbon emission from hydropower reservoirs represents a crucial integrant in global carbon cycling and has gained much more scholarly attention (Bastviken et al. 2011). Barros estimated the carbon emissions to be 48 Tg C/year as CO_2 and 3 Tg C/year as CH_4 from global hydroelectric reservoirs, which was clearly downgraded from earlier estimates due to taking into account the surface area (321 Tg of carbon per year for all types of reservoir). The GHG emission flux from hydropower reservoirs was 7.3 Tg C/year as CH_4 and 76 Tg C/year as CO_2 based on recently revised work (Hertwich 2013). This large range of estimates reflects both data paucity and inherent differences in the various methods for extrapolation. Thus, more detailed information for upscaling is needed when further testing global estimates at the regional level.

Although hydroelectricity is considered a substitute for high carbon-emitting coalfired generation, released greenhouse gases, especially CH_4 from the reservoirs, may impair the climate benefits. Research results based mainly on Brazilian hydropower reservoirs revealed that greenhouse gas emissions from hydropower may be comparable or higher than that from fossil-fuelled power stations under the same power capacity. Low greenhouse gases claims of the hydropower have been vitiated (Fearnside 2002). But, this view is still open for debate. The characteristics of the individual dam have a significant impact on the relative greenhouse gases emissions (Tremblay et al. 2005). However, the specific characteristics of the reservoir are not well reflected in some models (Delsontro et al. 2011; Sobek et al. 2003). Additionally, more dams will be constructed as a result of increased water demands due to continued population increase. Therefore it is essential to understand the effect that creating and maintaining dams has upon the global carbon cycle. Detailed and perfect models with robust, accurate and the widest coverage of circumstances, will play a key role when deciding to construct the additional hydro-power reservoirs in the future (Zhao et al. 2012). Most of all, the emission data obtained from representative reservoirs can calibrate the models.

The TGR on the Changjiang River in the Hubei province of China is the largest hydroelectric power station in the world, and it has the second-largest annual power output after Itaipu in Brazil. The TGR is a typical river-type reservoir with characteristics of rivers and lakes. There are certain differences between river-type reservoirs and normal reservoirs or lakes: the lengths of river-type reservoirs are much greater than their widths and depths, and they act as reservoirs during the dry seasons and as rivers during the flood seasons (Wang et al. 2009). Furthermore, the TGR includes 40 large reservoir-bays (watershed area > 100 km^2) and these bays' surface area accounts for 1/3 of the total surface area (Wang et al. 2010). When the TGR acts as a river in flood season, favorable hydrodynamic conditions and water quality appear in the main region of the reservoir,. However, flow velocities of tributaries near the reservoir are usually very slow because of the effects of the low discharge and high water level in the tributaries. With favorable sunlight, temperature, and wind speed conditions, algae are able to develop more easily, leading to eutrophication in these reservoir-bays. The balance of respiration and photosynthesis by phytoplankton along the water column in the TGR are inevitably influenced by the high spatial and temporal heterogeneity of the TGR aquatic ecosystem, thus manipulating the CO_2 concentration levels and the CO_2 flux at the water–air interface (Wang et al. 2009).

After the Three Gorges Dam was constructed, related research work conducted by national teams has provided some critical underlying information on the understanding of greenhouse gases emissions from the TGR (Xiao et al. 2013; Zhao et al. 2013; Zhao et al. 2012), but more thorough reservoir "greenhouse effect" assessments are still required. The goal of our study was to (1) explain the seasonal and spatial variation and the net balance of CO_2 flux between the reservoir and atmosphere, and (2) understand how the ecosystem processes regulate the CO_2 flux/$p$$CO_2$ variation in the TGR. The results of CO_2 diffusive emissions from the TGR are an attempt to improve the quality and quantity of available data, then provide support for ecological operations and decisions for similar river-type reservoirs.

2 Materials and methods

2.1 Study area

TGR (E106°50′–E110°50′, N29°16′–N31°25′) is one of the largest manmade lakes in the world, with a capacity of 3.93×10^{10} m^3 and a watershed area of over 1.00×10^6 km^2. The TGR is a river-type reservoir with a total surface area of 1084 km^2 (782 km^2 main steam and 302 km^2 tributary) when the water level is 175 m. The geography of the reservoir area is complex, with 74% being mountainous area, 21.7% being hilly area, only 4.3% being plain terrain in the river valley (Zhao et al. 2012), and 22.3% being forest coverage rate of the drainage area. The average wind speed is fairly constant and is about 1.2 m/s (Liu et al. 2016), and the mean annual temperature is

16.5–19 °C. Average annual precipitation is about 1100 mm with 80% falling in rainy seasons (Apr. to Oct.) (Ye et al. 2011). The Meixi River (N31°7′–N31°11′, E109°19′–E109°21′) rises in Fengjie County and has drainage in an area of 1932 km^2 before joining the Changjiang River. The main channel is 117 km long, and the total elevation fluctuation is 1610 m. Annual mean temperature is 16.5 °C, and the annual discharge of the river is 40.9 m^3/s in the catchment. More precipitation occurrs in the wet seasons, which last from May to September, and the mean annual value of 1151 mm. After operation of the Three Gorges Dam began, the Meixi River developed a perennial backwater area, which is located where the conflux area with the Changjiang River is and has a water surface of 8.7 km long.

After impoundment, the water residence time greatly differed within a year due to the TGR being operated in the mode of ‘‘storing clear and releasing muddy’’ water. During the flood seasons, the water residence time is less than 6 days maximum and more than 30 days during early summer period when the water level of the dam is drawn down to the minimum (145 m). Then, the ecosystem of the mainstream is more like a river system (Zhao et al. 2013). In the upper mainstem (310–660 km away from the dam), the water velocity remains above 2 m/s. In the 310 km stretch closest to the dam, the velocity is predicted to be about 0.5 m/s (Zhao et al. 2013). The flow velocity of its tributaries became very slow after the impounding of the TGR. Consequently, the phytoplankton in the tributaries may grow quickly, and the suitable water temperature, flow velocity, and other biological factors even can cause an “algae bloom” (Yang et al. 2012). Then, CO_2 can be fixed to organic carbon through photosynthesis, and the epilimnion is generally well aerated. Since the reservoir impounded in Jun. 2003, algal blooms frequently occur in its bays such as in the Meixi, Xiangxi, Daning, and Pengxi Rivers (Liu et al. 2016). Since the Meixi River is representated in most eutrophic bays of the TGR, CO_2 emissions from this river also should be of concern.

2.2 Sampling and analysis

Sampling sites are located at the upstream (MX03), middle reach (MX02), and downstream (MX01) of the tributary and the mainstream (Changjiang River; CJ01 and CJ02) in the central reservoir, respectively. Each month, we sampled the TGR in 2013 (*except for August, because of instrument repair*). Underway-pumping sampling began from the upstream (MX03) to middle reach (MX02), and finished at the estuary (MX01) (Fig. 1).

In each underway measurement, surface water was pumped into a barrel to continuously measure the physicochemical parameters such as water temperature (T), Chlorophyll a (Chl-a), and pH using a YSI-6600v2 and pCO_2 was determined using an automated analyzer equipped with a carbon dioxide sensor (Hydro C^{TM}/CO_2). In the Meixi River, a diving pump was used to pump deep water on board with the sampling interval of 5 m. The Hydro C^{TM}/CO_2 and YSI was also used to determine pCO_2 along the water column and in situ parameters. HCO_3^- was determined by titration with HCl in situ.

Based on a theoretical diffusion equation, the CO_2 flux (FCO_2) across the water–air interface can be estimated: (Soumis et al. 2008);

$$F = k(pCO_2\text{water} - pCO_2\text{air})K_H \tag{1}$$

where k is the piston velocity of CO_2, pCO_2 water is the partial pressure of CO_2 in the surface water, and pCO_2 air is the partial pressure of CO_2 in equilibrium with atmosphere. K_H is the solubility of CO_2 corrected using temperature (T) (Demarty and Bastien 2011).

$$\ln K_H = -58.0931 + 90.5069 \times (100/T) + 22.294 \times \ln(T/100) \tag{2}$$

Different basin physical factors can affect the k (cm/h) of CO_2 at the water–air interface but this is largely determined by wind speed and water turbulence (Alin et al. 2011). Considering the relatively low flow velocity in the Changjiang River (range from 0.049 to 0.809 m/s) and Meixi River (about 0.079 m/s) during the sampling period, the following equations were used to calculate the k (Borges et al. 2004; Crusius and Wanninkhof 2003; Soumis et al. 2008).

$$k = k_{600}\left(\frac{600}{Sc_T}\right)^{0.67} \tag{3}$$

$$Sc_T = 1911.1 - 118.11T + 3.45277T^2 - 0.04132T^3 \tag{4}$$

$$k600 = 2.07 + 0.215u_{10}^{1.7} \tag{5}$$

$$U10 = 1.22.U1 \tag{6}$$

where Sc_T is the Schmidt number for temperature T, k600 is the gas exchange coefficient normalized for CO_2 at 20 °C in fresh water with Schmidt number 600, U_{10} is the wind speed at 10 m above the water surface.

The TGR is a low-wind environment, with wind speeds below 2–3 m/s. In our study, the wind speed values were not directly determined but were instead based on the monthly average wind speeds in the sampling region (Fig. 2) (Yan et al. 2010).

After the operation of TGR began, three typical flow patterns of the Meixi River appear from the upstream to the estuary: the river pattern, the pattern of the transition zone from the river to the bay, and the pattern of the bay. The area was divided into three regions based on the three flow

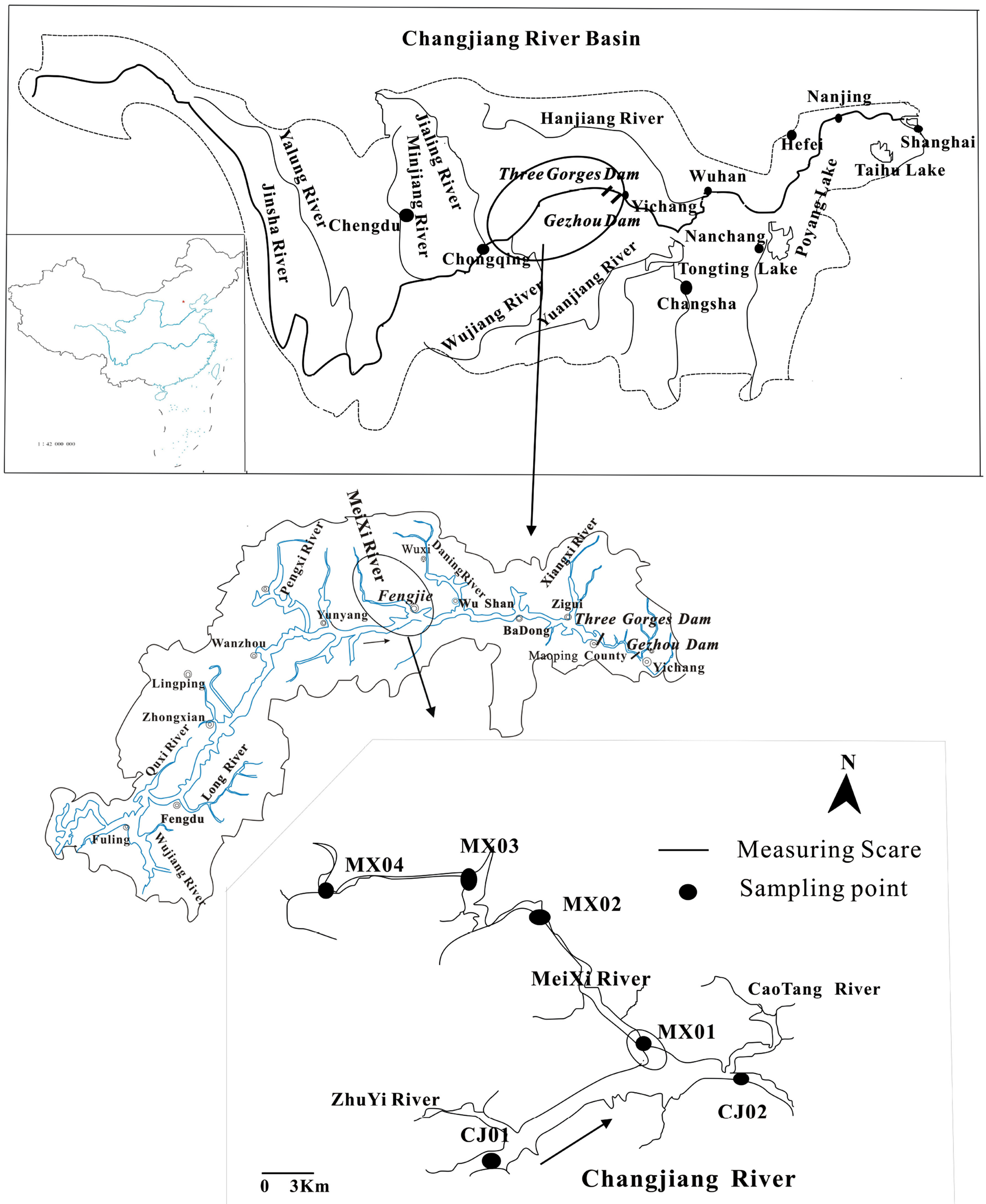

Fig. 1 The sampling sites of the study area

patterns (Li et al. 2014). The area of different regions was taken into account when estimating the mean CO_2 flux of the Meixi River. One-dimensional water flow pattern of the mainstream appears from the upstream to downstream of the dam (Li et al. 2002). Therefore, we used the mean fluxes of the CJ01 and CJ02 to estimate the average CO_2 flux of the mainstream. The estimation of the diffusion flux does not take the variation of water surface area into account, so this may produce some uncertainty in the calculations.

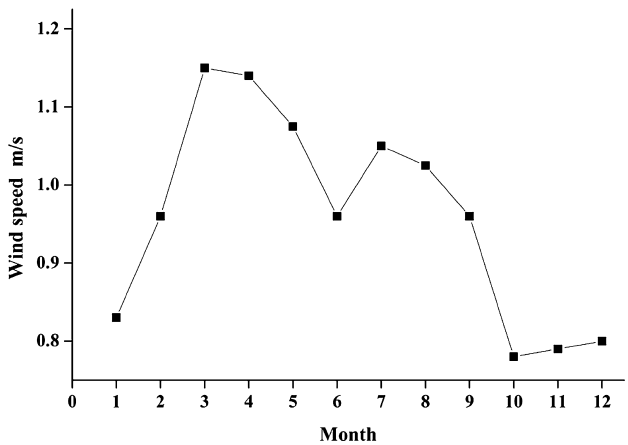

Fig. 2 The monthly average wind speeds in Chongqing from 1961 to 2007. (Fengjie, a County of Chongqing)

3 Results and discussion

3.1 Spatial variation of water temperature and turbidity

In the TGR mainstream, the mean water temperature of CJ01 and CJ02 was 19.65 and 20.68 °C, ranging from 13.07 to 24.92 and 13.01 to 25.15 °C, respectively. The water temperature of the surface water in the Meixi River ranged from 13.07 °C in the winter to 28.75 °C in the summer, with an average of 21.5 °C. An obvious temperature discontinuity (more than 5 °C) developed between the mainstream and the tributary in July. As can be seen from Fig. 3a, at the transitional zone (about 0–4 km), the water temperature in the surface water showed an increasing pattern except in December, which was caused by the backflow of mainstream. The temperature in the middle of the Meixi river remained relatively steady but higher than that in the upper and lower reaches of Meixi river. The water temperature of the mainstream remained basically stable from the CJ01 to CJ02 of the study area. The data shown in the figures of the mainstream comes from the average of the two sampling points in TGR. Results show that the water body in the mainstream was as a complete mixing pattern (river-type) most of the year. The flow velocity of the TGR mainstream was too fast and turbulent mixing was too rigorous to develop the stratification. In addition, the development of stratification also can be limited by short residence time. As a result, the mainstream has no thermal stratification during the whole year.

Different to the mainstream, the water columns for Meixi River were stratified throughout the summer and were not stratified between Oct–Dec, Jan–Feb. As can be seen from Fig. 3c, there were three different patterns based on monthly surveys: (1) transition period when the water column transformed from mixing to stratification (from Mar. to May), (2) stratification period when the stratification condition could be observed discontinuously (from May to Sep.). The flow velocity in the Meixi River near the reservoir was usually very slow because of the effects of the high water level of the mainstream and low discharge in the tributaries. The low flow velocity and warm air temperatures of late spring and summer contributed to a strong thermal stratification of the Meixi River. The thermal stratification of Meixi Bay created a layer of warm water, the epilimnion, (MX01:27.00 °C, MX02:27.65 °C, MX03:29.30 °C, Jul.) and a layer of cold water, the hypolimnion, (MX01:24.52 °C, MX02:24.90 °C, MX03:24.92 °C, Jul.). A strong temperature gradient of the thermocline prevented the epilimnion from mixing any deeper, thus isolating the hypolimnion waters from the water body's surface (Nõges et al. 2010). The Meixi river may be considered to have a well-developed stratification due to the prolonged residence time during the warm seasons. (3) The mixing period (from October, to March next year, when water column was completely mixed).

The turbidity was found to have a significant temporal and spatial variation in the TGR. From May to September, low transparency (high turbidity) occurred in the study area when major inflows and rainfall events happened (Fig. 3b). The drainage basin input particles through surface runoff, thus decreasing the transparency but increasing the dissolved and particulate allochthonous carbon. These degradable organic carbons enhanced CO_2 production and this stock of organic matter was subsequently submerged and oxidized during the high-water stage, leading to high pCO_2. In addition, higher decomposition rates of organic carbon were caused by the higher water temperature during this period, and the temperature dependence can explain why pCO_2 was lower during cold seasons (Oct. to Dec., Jan. to Feb.) in the mainstream. But, in highly transparent lakes, photosynthesis was supported in the epilimnion where light could possibly penetrate (Nõges et al. 2010) and photosynthetic uptake of CO_2 could reduce the net flux. In the Meixi Bay, the stratification along the water column provided ample light for phytoplankti to develop during warm seasons (Jul. to Sep). Thus, the pCO_2 was much lower during warm seasons.

3.2 Variations of chlorophyll-a and dissolved oxygen in the TGR

Chl-a is a main pigment for photosynthetic process in phytoplankton and through its analysis, either amount of biomass can be estimated or can be considered as an index for the trophic level of aquatic ecosystem. The phytoplankton biomass (represented as Chl-a) was higher in the Meixi River than that in the mainstream, and it varied from 0.38 to 28.13 μg/L. In March, most of the tributary surface

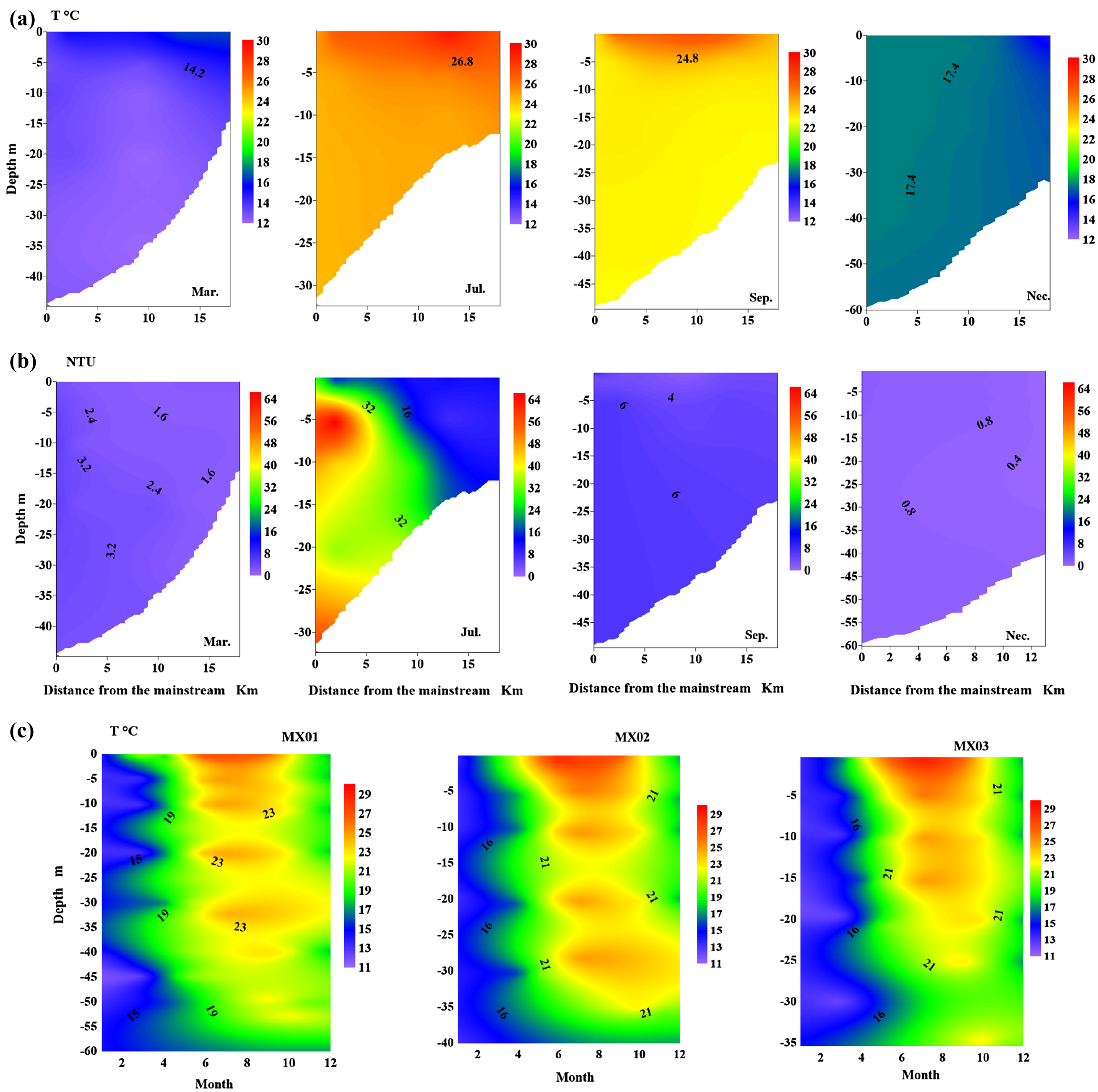

Fig. 3 Temporal and spatial variation in temperature (**a**), (**c**) and turbidity (**b**) at the TGR

has Chl-a concentrations smaller than 2 μg/L. In the following months (Apr to Jul), the Chl-a concentration increased and the upper and lower reaches of the river were dominated by values above 5 μg/L. However, the middle of the river and the estuary returns to chlorophyll-a concentration below 3 μg/L. In September, the main body of the tributary, from upstream to downstream, showed concentrations up to 25 μg/L. In December, the Mei River displays a high Chl-a concentration, whose values are far below 1 μg/L. The mainstream showed basically consistent Chl-a concentrations between 0.26 and 4.6 μg/L with no pronounced seasonality (Fig. 4a). Although nutrient contents were high, Chl-a was usually lower than 5 μg/L and no algal bloom occurred in the mainstream (Yang et al. 2010). Phytoplankton growth was prevented by high flow velocity due to the short residence time during spring and summer, which were the seasons of algal growth in the mainstream (Xu et al. 2011). Thus, phytoplankton may be insignificant in the C dynamics in the mainstream of the TGR. However, the situation in the Meixi River was different because of its prolonged residence time, thermal stratification, and extremely small velocities. The slow

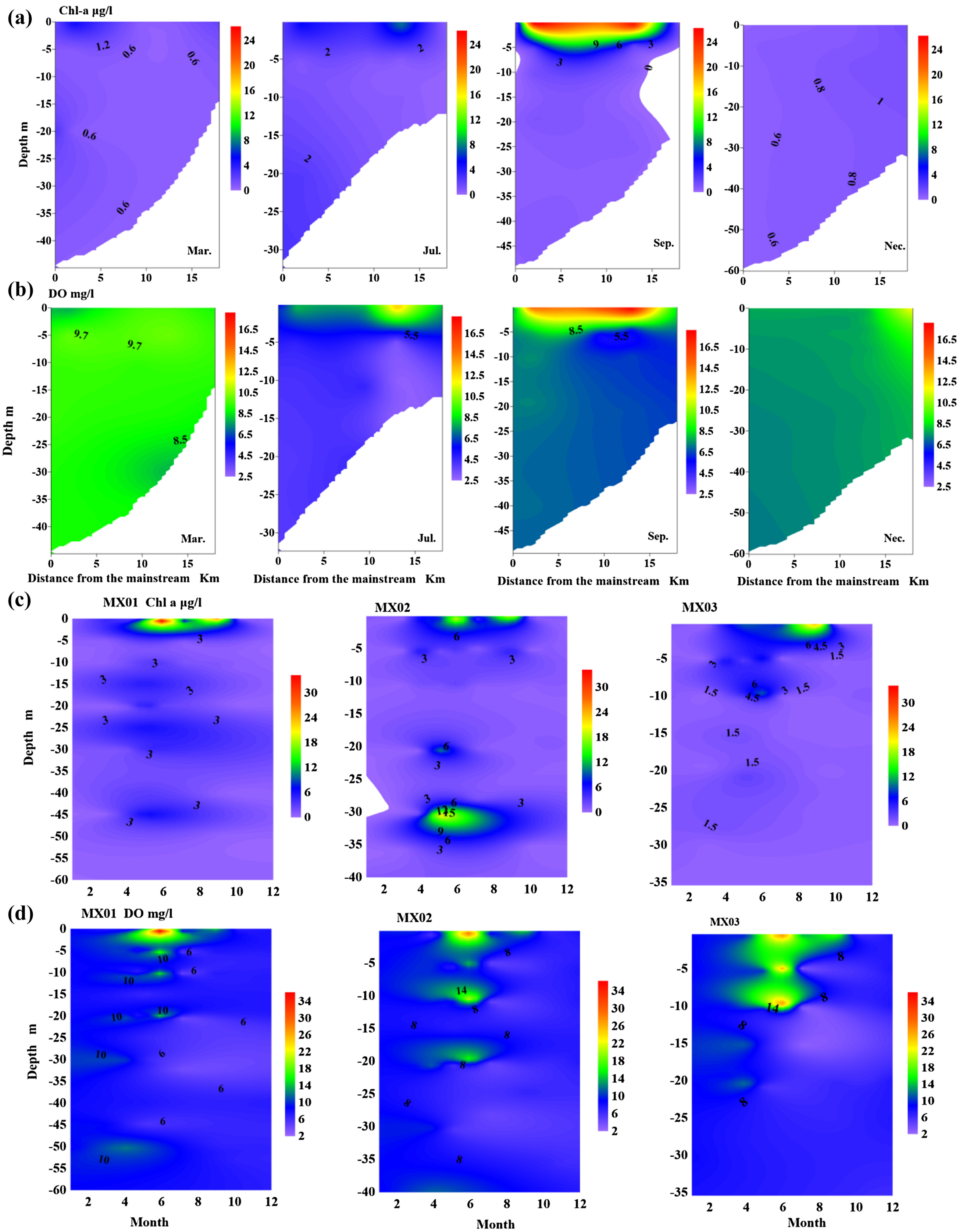

Fig. 4 Temporal and spatial variation in Chl-a (**a**), (**c**) and DO (**b**), (**d**) concentration in the TGR

flow-velocity, long residence time, relatively high water transparency, and high stratification provide the right environment for aqueous biogenic activities. Coupled with TN, TP, and other nutrients in the bay accumulate, algae grew rapidly, and Chl-a concentration rose rapidly. The highest Chl-a concentration (5.4–24.62 μg/L; Fig. 4c) was seen during the warm seasons (Jul. to Oct.) with lower water turbidity (2.96–13.37 NTU) than that during the cold seasons (Chl-a: 0.64–1.04 μg/L), suggesting that the aquatic environment promoted the growth of phytoplankton during this period.

The spatial–temporal variation of DO was the same with those of Chl-a along the Meixi River (Fig. 4b). In the Meixi River, the DO levels decreased from 9.06 (Jan.) to 7.75 (Apr.) mg/L and from 16.25 (Sep.) to 7.74 (Dec.) mg/L, suggesting dominant heterotrophic activity. During the spring to autumn period, photosynthesis prevailed in the water, and the epilimnion was supersaturated with DO, ranging from 7.75 mg/L (Apr.) to 16.25 mg/L(Sep.). During the cold seasons, the collapse of thermal stratification could result in the disappearance of the stratification of DO (Fig. 4b, d).

3.3 Variations in pH and pCO_2 in the TGR

The average pH across the mainstream and the Meixi River was 7.95 and 8.49, respectively. As the above result shows, the turbidity depressed distinctly and Chl-a, DO increased from the mainstream to the Meixi River. The variation in pH was identical with that of Chl-a along the Meixi River, and high pH was often associated with supersaturated DO. At the region of the transition zone, the concentration of the Chl-a, DO, and pH had been changed obviously due to the interactions of the mainstream and the tributary (Fig. 5a). In the Meixi River, pH showed a declining trend due to the greater respiration during the cold seasons and an increasing trend during the warm seasons, which was consistent with a increased net ecosystem production (Fig. 5c). The higher pH occurred from June to September (8.43–9.24) and then decreased by December (8.38). The increase from 8.43 to 9.24 in pH during the warm seasons was associated with a high Chl-a concentration. Increasing the dissolved oxygen to oversaturation indicated that enhancing the photosynthetic intensity can lead to pH increase. The low pH levels during the cold seasons was associated with low Chl-a concentration and oxygen levels, suggesting that significant organic matter decomposition led to a decrease in pH.

On the contrary, the pCO_2 decreased gradually from the estuary to the Meixi River. In the confluent area, higher pCO_2 was measured at the water surface. After the confluent area, the pCO_2 decreased and was even lower than that in the atmosphere, which corresponded to high concentrations of DO and Chl a, representing the prevalence of primary production in the epilimnion. However, there was no obvious longitudinal variation of pCO_2 along the the Meixi River during the cold seasons (Fig. 5b). The average pCO_2 in the mainstream was 1558.7 μatm, a value that was far away the atmospheric CO_2 (394 μatm) (Panneer Selvam et al. 2014), with a range from 704 to 2646 μatm. The Meixi River as well as the mainstream had high pCO_2, that varied from 500 to 1781 μatm due to the high occurrences of respiration/decomposition along the water column in the cold seasons. Significant differences in pCO_2 levels were found during the warm seasons, resulting in significantly lower pCO_2 values (from 143.1 to 271.5 μatm) in the Meixi River, which was associated with a high Chl-a concentration. During this period the high phytoplankton biomass, and therefore high primary production, led to low pCO_2 levels in the epilimnion and high pCO_2 levels in the hypolimnion, which was attributed to the mineralisation of organic matter. In late autumn, the decreasing temperature and impoundment of the TGR destroyed the stable stratification. Until the following spring, a vertical stratification of pCO_2 was created with increasing water temperature, recovery of planktonic and microbial activities, and then the stratification prevented the water column from mixing (Fig. 5b).

In the Meixi Bay, pCO_2 declined due to biological uptake during the warm seasons when net photosynthesis was expected to be greatest. However, during the winter, the heterotrophic respiration by phytoplankton prevailed in the water due to the limitation of light and temperatures, resulting in higher pCO_2 (Fig. 5d). Additionally, the sediment, nutrients, and buried organic matter could be potentially decomposed by pelagic bacteria and transferred from the bottom of the Meixi River to the surface via mixing, resulting in higher pCO_2. In contrast, the mainstream showed no seasonal variations in Chl-a concentrations and had higher pCO_2.

3.4 CO_2 emissions from the TGR

The area-weighted average CO_2 flux was 11.4 mg/m^2 h of the Meixi River, and the annual average CO_2 flux was 50.0 mg/m^2 h of the mainstream. Figure 6 shows that the mainstream had high positive FCO_2 throughout the year as it ranged from 26.1 mg/m^2 h (Jan.) to 92.2 mg/m^2 h (Jul.). The surface water was a source of CO_2 for the atmosphere throughout the year. However, in the Meixi River, the CO_2 fluxes were negative from April (−3.4 mg/m^2 h) to September (−10.9 mg/m^2 h). During this period, CO_2 was absorbed by photosynthesis, leading to the CO_2 infiltration of the water from the atmosphere. The minimum CO_2 flux occurred in September and had a value of −10.9 mg/m^2 h, representing an significant invasion of atmospheric CO_2.

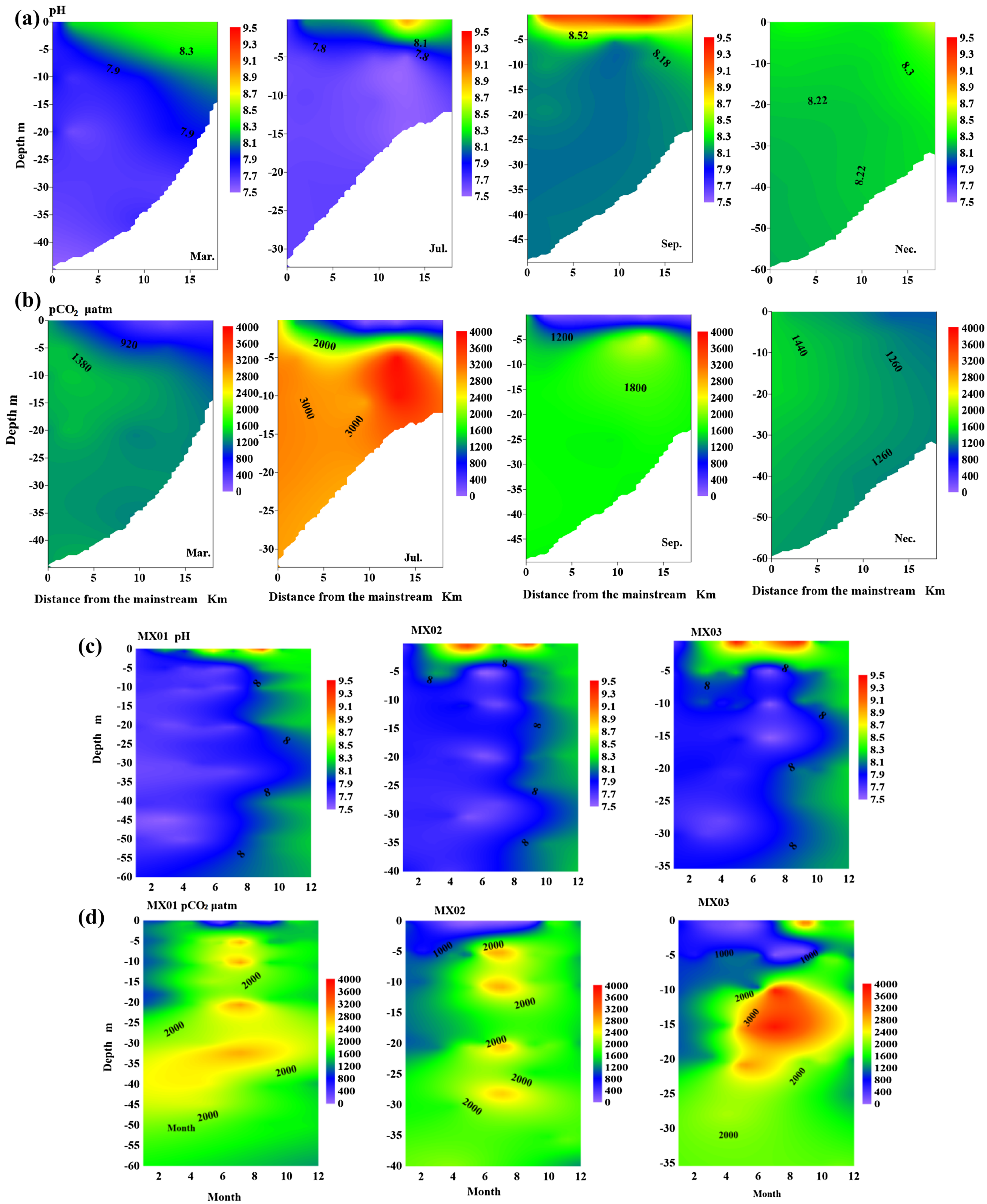

Fig. 5 Temporal and spatial variation in pH (**a**), (**c**) and pCO_2 (**b**), (**d**) at the TGR

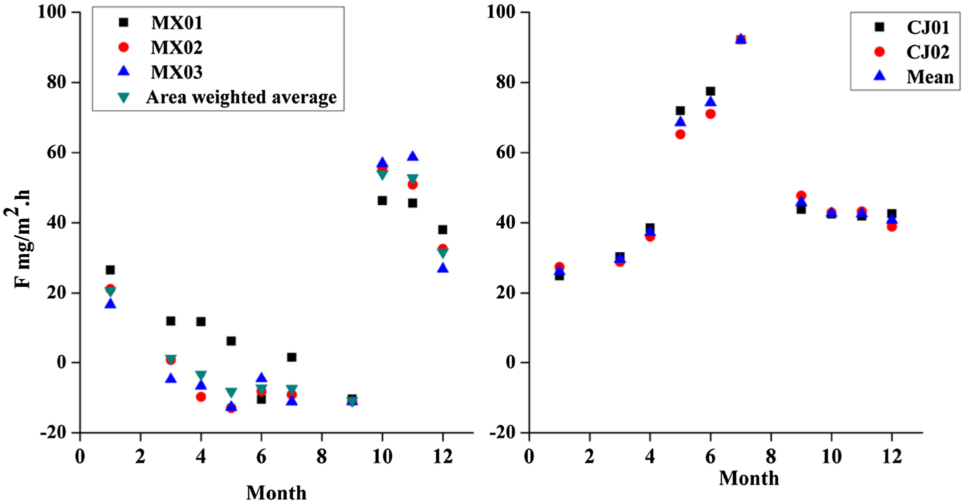

Fig. 6 Diffusion fluxes of CO_2 from the Changjiang and the Meixi river, 2013

During the cold seasons, the Meixi River also had positive FCO_2 with the highest value of 53.4 mg/m^2 h in October. The surface water of the Meixi River acted as sources or sinks of CO_2.

The results of variability in the same reservoir may have resulted from the different methods used to measure CO_2 flux. Our results, which were obtained through calculations based on equations for diffusion at the water–air interface, were much lower than those obtained with static chambers by Zhao, Yang, etc. (e.g., 176 and 163 mg/m^2 h, respectively) (Yang et al. 2013; Zhao et al. 2013). The CO_2 flux rates obtained with SC were highly variable within sites, measured time, and they showed no spatial autocorrelation. Factors such as chamber operation, sampling time and location, sample storage or problems in the gas analysis all can increase the uncertainties in the flux estimation (Christiansen et al. 2011). In Zhao and Yang's studies, the air samples were manually collected at 10 min intervals after the deployment. The long interval time for sampling may have overestimated the CO_2 flux. Furthermore, this study used an online system to determine the pCO_2 in water at the main stream and tributary of the TGR, thus improving the sampling density. Soumis et al. (2008) estimated an average of CO_2 flux $\sim$58 mg/m^2 h and 146 from temperate and tropical hydroelectric reservoirs, respectively. Also, an average of CO_2 flux estimated by Barros was 16 mg/m^2 h from temperate reservoirs (Li and Zhang 2014). Our estimated CO_2 efflux (50 mg/m^2 h of the mainstream and 11.4 mg/m^2 h of the tributary, respectively) from the TGR surface area was in agreement but previous results were higher and better matched the tropical reservoirs. Greenhouse gases emissions from aquatic systems were due to the degradation of the organic matter present in or entering the systems. The average CO_2 flux of the Global river was 55 mg/m^2 h. Tropical reservoirs generally had high organic matter content, high temperature, and an anoxic bottom layer, all contributing to Greenhouse gas (CO_2 and CH_4) production (Demarty and Bastien 2011). Most large rivers, such as the Parana, Amazon, have higher pCO_2 than atmospheric CO_2 levels due to internal microbial respiration of the riverine organic matter (Depetris and Kempre 1993). High pCO_2 translated to large CO_2 evasion fluxes from water to atmosphere. Previous measurements in the TGR illustrated that pCO_2 in the mainstem of the Changjiang River was close to 5000 µatm (Zhao et al. 2013). This pCO_2 level was higher than that of the Amazon (4350 $\pm$ 1900 atm), but dissolved organic carbon (108 µmol/L) of the Changjiang River was lower than that of the Amazon (averaged from 333 to 500 µmol/L in the mainstem). (Cole et al. 2001; Marcelino et al. 2015; Richey and Forsberg 1990; Wu et al. 2007). This indicates that previous studies may have overestimated the CO_2 evasion from the TGR. In addition, when compared to other reservoirs worldwide, our estimated CO_2 emission flux was similar to other temperate reservoirs but far below the CO_2 fluxes of tropical reservoirs (Table 1).

Although previous studies overestimated the CO_2 evasion, the results still show that the average CO_2 fluxes remain basically stable from upstream to downstream of the dam (Table 2). The focus of our work is about the difference between the mainstream and tributaries, so small changes in CO_2 fluxes of the mainstream from the upstream to the downstream can be ignored. A one-dimensional mathematical model has been applied to calculate the holistic hydraulic characteristics in the natural condition of the TGR (Wu 2013; Zhang et al. 2006). Therefore, using the results in our study to estimate the CO_2 efflux from the reservoir was feasible in practice and worthy of research and dissemination. In addition, the surface water of the mainstream is a source of CO_2 for the atmosphere throughout the year. However, the surface

Table 1 CO_2 flux of the reservoirs in other temperature zones

Location	Reservoirs	CO_2 flux [mg CO_2/(m^2 h)]	
		Mean	Range
Boreal			
	Robert-Bourassa (Demarty et al. 2011)	27.5	1.9–271.2
Temperate			
USA	Shasta (Soumis et al. 2005)	52.0	14.6–89.6
	Oroville (Soumis et al. 2005)	42.8	11.1–101.2
China	TGR[a]	50.0	26.1–92.2
	TGR (Zhao et al. 2012)	176	
	MeiXi River[a] (a tributary of TGR)	11.4	−10.9 to 53.4
Tropical			
Brazil	Miranda (dos Santos et al. 2006)	182.83	0.67–2549
	Três Marias (dos Santos et al. 2006)	46.4	1.38–419.2
	Samuel (dos Santos et al. 2006)	310.3	91.67–1011.8
	Balbina (Kemenes et al. 2011)	576.88	52.42–1303.04
French	Petit Saut (Abril et al. 2005)	240.17	–18.33 to 660

[a] This study

Table 2 Annual average CO_2 flux from different sampling sites of TGR

Location	Distance from the dam km	Annual mean CO_2 flux mg/m^2 h
Mainstream		
BaDong	75	231 ± 146.67 (Zhao et al. 2013)
WuShan	124	231 ± 201.67 (Yang et al. 2013)
WanZhou	282	231 ± 201.66 (Zhao et al. 2013)
QinXi	467	232.83 ± 104.5 (Zhao et al. 2012)
CunTan	590	311.67 ± 177.8 (Zhao et al. 2012)

water of the tributary acts as both sources and sinks of CO_2. Therefore, the CO_2 efflux from the mainstream and tributaries should be estimated separately when estimating the total CO_2 emission from the TGR surface. Considering the area of 782 km^2, the total diffusive CO_2 flux from the mainstream was 0.34 Tg CO_2/year and 0.03 Tg CO_2/year from the tributaries, when considering the total area of 302 km^2. The total diffusive CO_2 emission from the TGR was estimated to be 0.37 Tg CO_2/year.

4 Conclusion

Our analysis shows that the TGR emitted CO_2 to the atmosphere and that these emissions were 0.37 Tg/year. The emission rates of CO_2 from the reservoir surface varied from 26.1 to 92.2 mg/m^2 h with an mean value of 50.0 mg/m^2 h (mainstream) and −10.9 to 54.0 mg/m^2 h with an mean value of 11.4 mg/m^2 h (tributary). This emission flux (boundary layer equations measurements) was lower than previously estimated (static chamber measurements) but in agreement with the average CO_2 flux from temperate reservoirs (25°–50° latitudinal belt) (Barros et al. 2011). Our estimated CO_2 emission flux was similar to other temperate reservoirs but much lower than that of the tropical reservoirs. In addition, a higher flow velocity and a large amount of allochthonous import caused relatively higher CO_2 fluxes year round in the mainstream. However, the surface water of the tributaries can also act as a sink of CO_2 for atmosphere Therefore, the spatial and temporal heterogeneity should be taken into account when studying similar river-type reservoirs in the future.

Acknowledgements The authors thank every colleague for their full assistance in field sampling. We also appreciate the reviewers for their valuable comments on this manuscript. This study was funded by the National Natural Science Foundation of China (No. 41573064), The National Key Research and Development Program of China (No. 2016YFA0601003, and the Special S&T Project on Treatment and Control of Water Pollution (No. 2012ZX07104-001).

References

Abril G, Guérin F, Richard S, Delmas R, Galy-Lacaux C, Gosse P, Tremblay A, Varfalvy L, Dos Santos MA, Matvienko B (2005) Carbon dioxide and methane emissions and the carbon budget of a 10-year old tropical reservoir (Petit Saut, French Guiana). Glob Biogeochem Cycl 19(4):n/a–n/a

Alin SR, Salimon CI, Richey JE, Holtgrieve GW, Krusche AV, Anond S (2011) Physical controls on carbon dioxide transfer velocity and flux in low-gradient river systems and implications for regional carbon budgets. J Geophys Res Biogeosci 116(G1):248–255

Barros N, Cole JJ, Tranvik LJ, Prairie YT, Bastviken D, Huszar VLM, del Giorgio P, Roland F (2011) Carbon emission from hydroelectric reservoirs linked to reservoir age and latitude. Nat Geosci 4(9):593–596

Bastviken D, Tranvik LJ, Downing JA, Crill PM, Enrich-Prast A (2011) Freshwater methane emissions offset the continental carbon sink. Science 331:50

Borges AV, Vanderborght J-P, Schiettecatte L-S, Gazeau F, Ferrón-Smith S, Delille B, Frankignoulle M (2004) Variability of the gas transfer velocity of CO_2 in a macrotidal estuary (the Scheldt). Estuaries 27(4):593–603

Christiansen JR, Korhonen JFJ, Juszczak R (2011) Assessing the effects of chamber placement, manual sampling and headspace mixing on CH_4 fluxes in a laboratory experiment. Plant Soil 343(1):171–185

Cole JJ, Caraco NF, Cole JJ, Caraco NF (2001) Mar Freshw Res 52(1):101

Cole JJ, Prairie YT, Caraco NF, McDowell WH, Tranvik LJ, Striegl RG, Duarte CM, Kortelainen P, Downing JA, Middelburg JJ, Melack J (2007) Plumbing the global carbon cycle: integrating inland waters into the terrestrial carbon budget. Ecosystems 10(1):172–185

Crusius J, Wanninkhof R (2003) Gas transfer velocities measured at low wind speed over a lake. Limnol Oceanogr 48(3):1010–1017

Delsontro T, Kunz MJ, Kempter T, Wüest A, Wehrli B, Senn DB (2011) Spatial heterogeneity of methane ebullition in a large tropical reservoir. Environ Sci Technol 45(23):9866–9873

Demarty M, Bastien J (2011) GHG emissions from hydroelectric reservoirs in tropical and equatorial regions: review of 20 years of CH4 emission measurements. Energy Policy 39(7):4197–4206

Demarty M, Bastien J, Tremblay A (2011) Annual follow-up of gross diffusive carbon dioxide and methane emissions from a boreal reservoir and two nearby lakes in Québec, Canada. Biogeosciences 8(1):41–53

Depetris PJ, Kempre S (1993) Carbon dynamics and sources in the Parani River. Limnol Oceanogr 38(2):382–395

dos Santos MA, Rosa LP, Sikar B, Sikar E, dos Santos EO (2006) Gross greenhouse gas fluxes from hydro-power reservoir compared to thermo-power plants. Energy Policy 34(4):481–488

Fearnside PM (2002) Greenhouse gas emissions from a hydroelectric reservoir (Brazil's Tucuruí Dam) and the energy policy implications. Water Air Soil Pollut 133(1):69–96

Hertwich EG (2013) Addressing biogenic greenhouse gas emissions from hydropower in LCA. Environ Sci Technol 47(17): 9604–9611

Kemenes A, Forsberg BR, Melack JM (2011) CO_2 emissions from a tropical hydroelectric reservoir (Balbina, Brazil). J Geophys Res Biogeosci 116(G3):209–216

Li S, Zhang Q (2014) Partial pressure of CO_2 and CO_2 emission in a monsoon-driven hydroelectric reservoir (Danjiangkou Reservoir), China. Ecol Eng 71:401–414

Li JX, Liao WG, Huang ZL (2002) Prediction of the impact of Three Gorges Project on water flow and water quality in the reservoir. Water Resour Hydropower Eng 33:22–26

Li Z, Bai L, Gao JS, Fang F, Jiang T (2013) Comparative study on water–air CO_2, CH4 flux in two tributaries in the Three Gorges Reservoir, China. Environ Sci 34(3):1008–1016

Li S, Wang YC, Cao M, Qian HJ, Xu T, Zhou ZR, Wang FS (2014) Partial pressure and diffusion flux of dissolved carbon dioxide in the mainstream and tributary of the central Three Gorges Reservoir in summer. Environ Sci 35(3):885–891 (**in Chinese**)

Liu D, Yang Z, Daobin JI, Jun MA, Cui Y, Song L (2016) A review on the mechanism and its controlling methods of the algal blooms in the tributaries of Three Gorges Reservoir. J Hydraul Eng 47(3):443–454

Marcelino AA, Santos MA, Xavier VL, Bezerra CS, Silva CR, Amorim MA, Rodrigues RP, Rogerio JP (2015) Diffusive emission of methane and carbon dioxide from two hydropower reservoirs in Brazil. Braz J Biol 75(2):331–338

Nõges P, Poikane S, Kõiv T, Nõges T (2010) Effect of chlorophyll sampling design on water quality assessment in thermally stratified lakes. Hydrobiologia 649(1):157–170

Panneer Selvam B, Natchimuthu S, Arunachalam L, Bastviken D (2014) Methane and carbon dioxide emissions from inland waters in India—implications for large scale greenhouse gas balances. Glob Change Biol 20(11):3397–3407

Raymond PA, Hartmann J, Lauerwald R, Sobek S, McDonald C, Hoover M, Butman D, Striegl R, Mayorga E, Humborg C, Kortelainen P, Durr H, Meybeck M, Ciais P, Guth P (2013) Global carbon dioxide emissions from inland waters. Nature 503(7476):355–359

Regnier P, Friedlingstein P, Ciais P, Mackenzie FT, Gruber N, Janssens IA, Laruelle GG, Lauerwald R, Luyssaert S, Andersson AJ, Arndt S, Arnosti C, Borges AV, Dale AW, Gallego-Sala A, Goddéris Y, Goossens N, Hartmann J, Heinze C, Ilyina T, Joos F, LaRowe DE, Leifeld J, Meysman FJR, Munhoven G, Raymond PA, Spahni R, Suntharalingam P, Thullner M (2013) Anthropogenic perturbation of the carbon fluxes from land to ocean. Nat Geosci 6(8):597–607

Richey JE, Forsberg BR (1990) Biogeochemistry of carbon in the Amazon River. Limnol Oceanogr 35(2):352–371

Richey JE, Melack JM, Aufdenkampe AK, Ballester VM, Hess LL (2002) Outgassing from Amazonian rivers and wetlands as a large tropical source of atmospheric CO_2. Nature 416(6881): 617–620

Sobek S, Algesten G, Bergstrom A-K, Jansson M, Tranvik LJ (2003) The catchment and climate regulation of pCO_2 in boreal lakes. Glob Change Biol 9(4):630–641

Soumis N, Lucotte M, Canuel R, Weissenberger S, Houel S, Larose C, Duchemin É (2005) Hydroelectric reservoirs as anthropogenic sources of greenhouse gases. Water Encycl 3:203–210

Soumis N, Canuel R, Lucotte M (2008) Evaluation of two current approaches for the measurement of carbon dioxide diffusive fluxes from lentic ecosystems. Environ Sci Technol 42(8): 2964–2969

St. Louis VL, Kelly CA, Duchemin E, Rudd JWM, Rosenberg DM (2000) Reservoir surfaces as sources of greenhouse gases to the atmosphere: a global estimate. Bioscience 50(9):766

Tremblay A, Varfalvy L, Roehm C, Garneau M (eds) (2005) Greenhouse gas emissions–fluxes and processes: hydroelectric reservoirs and natural environments, Apress 7(2):111–127

Wang L-L, Yu Z-Z, Dai H-C, Cai Q-H (2009) Eutrophication model for river-type reservoir tributaries and its applications. Water Sci Eng 2(1):16–24

Wang L, Cai Q, Xu Y, Kong L, Tan L, Zhang M (2010) Weekly dynamics of phytoplankton functional groups under high water level fluctuations in a subtropical reservoir-bay. Aquat Ecol 45(2):197–212

Wenjun W (2013) Change of channel conditions of the reach from Wanzhou to Fuling in the Yangtze River at incipient stage of Three Gorges Reservoir. J Chongqing Jiaotong Univ (Natural Science) 3:024

Wu Y, Zhang J, Liu SM, Zhang ZF, Yao QZ, Hong GH, Cooper L (2007) Sources and distribution of carbon within the Yangtze River system. Estuar Coast Shelf Sci 71(1):13–25

Xiao S, Wang Y, Liu D, Yang Z, Lei D, Zhang C (2013) Diel and seasonal variation of methane and carbon dioxide fluxes at Site Guojiaba, the Three Gorges Reservoir. J Environ Sci 25(10):2065–2071

Xu Y, Zhang M, Wang L, Kong L, Cai Q (2011) Changes in water types under the regulated mode of water level in Three Gorges Reservoir, China. Quat Int 244(2):272–279

Yan LI, Dan G, Dong XN, Yan Z (2010) Climate change of wind speed in chongqing from 1961 to 2007. Trans Atmospheric Sci 33(3):336–340 (**in Chinese**)

Yang Z, Liu D, Ji D, Xiao S (2010) Influence of the impounding process of the Three Gorges Reservoir up to water level 172.5 m on water eutrophication in the Xiangxi Bay. Sci China Technol Sci 53(4):1114–1125

Yang ZJ, Liu DF, Ma J, Chen YY, Fang XF, Ji DB (2012) Effects of special vertical layered water temperatures on algal bloom in Xiangxi Bay of Three Gorges Reservoir. Eng J Wuhan Univ 45(1):1–9

Yang L, Lu F, Wang X, Duan X, Tong L, Ouyang Z, Li H (2013) Spatial and seasonal variability of CO_2 flux at the air–water interface of the Three Gorges Reservoir. J Environ Sci 25(11):2229–2238

Ye C, Li S, Zhang Y, Zhang Q (2011) Assessing soil heavy metal pollution in the water-level-fluctuation zone of the Three Gorges Reservoir, China. J Hazard Mater 191(1–3):366–372

Zhang Z, Long TY, Chen-Yong GU, Lan K, Zeng J (2006) One-dimensional water flow modeling for Chongqing region at two typical storage levels in the Three-Gorges Reservoir. J Chongqing Univ 29(8):13–14

Zhao Y, Wu BF, Zeng Y (2012) Spatial and temporal aspects of greenhouse gas emissions from Three Gorges Reservoir, China. Biogeosci Discuss 9(10):14503–14535

Zhao Y, Wu BF, Zeng Y (2013) Spatial and temporal patterns of greenhouse gas emissions from Three Gorges Reservoir of China. Biogeosciences 10(2):1219–1230